International Journal of Fluid Machinery and Systems
Vol. 4, No. 3, July-September 2011

DOI: 10.5293/IJFMS.2011.4.3.307
ISSN (Online): 1882-9554

Original Paper

Vortex Features in a Half-ducted Axial Fan with Large Bellmouth (Effect of Tip Clearance)

Norimasa Shiomi[1], Yoichi Kinoue[1], Toshiaki Setoguchi[1] and Kenji Kaneko[1]

[1]Department of Mechanical Engineering, Saga University
1 Honjo-machi, saga, 840-8502, Japan, siomi@me.saga-u.ac.jp, kinoue@me.saga-u.ac.jp, setoguci@me.saga-u.ac.jp, kaneko-k@po.bunbun.ne.jp

Abstract

In order to clarify the features of tip leakage vortex near blade tip region in a half-ducted axial fan with large bellmouth, the experimental investigation was carried out using a 2-dimensional LDV system. Three sizes of tip clearance (TC) were tested: those sizes were 1mm (0.55% of blade chord length at blade tip), 2mm (1.11% of blade chord length at blade tip) and 4mm (2.22% of blade chord length at blade tip), and those were shown as TC=1mm, TC=2mm and TC=4mm, respectively. Fan characteristic tests and the velocity field measurements were done for each TC. Pressure – flow-rate characteristics and two-dimensional velocity vector maps were shown. The vortex trace and the vortex intensity distribution were also illustrated. As a result, a large difference on the pressure – flow-rate characteristics did not exist for three tip clearance sizes. In case of TC=4mm, the tip leakage vortex was outflow to downstream of rotor was not confirmed at the small and reference flow-rate conditions. Only at the large flow-rate condition, its outflow to downstream of rotor existed. In case of TC=2mm, overall vortex behaviors were almost the same ones in case of TC=4mm. However, the vortex trace inclined toward more tangential direction. In case of TC=1mm, the clear vortex was not observed for all flow-rate conditions.

Keywords: Tip leakage vortex, Tip clearance, Ventilation fan, LDV measurement

1. Introduction

In many case, a room ventilation fan is equipped in a kitchen of Japanese house. In Japanese house, there is a one large space called “LDK” including a Living, a Dinning room and a Kitchen. In such a space, the sound from a room ventilation fan in a kitchen becomes the noise for the people in a living room. Therefore, it is desired that the sound from a room ventilation fan is low noise level. A low-pressure axial fan is often used as a room ventilation fan because its structure is simple and its manufacturing and maintaining cost are low. In this usage, the upstream and downstream space of a fan is open air without connecting the duct.

The fan noise is roughly classified into the mechanical noise and aerodynamics noise. It is well- known that the aerodynamics noise is mainly caused by the vortices in flow fields. Inoue [1] stated that the turbomachinery was vortex generator. In turbo machinery, many types of vortex exist, e.g. tip leakage vortex, leading edge separation vortex, house-shoe vortex, hub-corner separation vortex, passage secondary vortex and so on. In these vortices, it is generally known that the tip leakage vortex has a large effect on fan performance, for example, efficiency, pressure-rise characteristic, and fan noise. Therefore, many researches for the natures of tip leakage flow and vortex have been conducted.

Lakshminarayana [2] reported the effect of tip clearance flow on axial flow turbomachine, and he proposed the vortex model to simulate the flow field including the tip leakage vortex. The experimental study on tip leakage vortex was carried out by Inoue et al. [3] to clarify the structure and behavior of tip leakage vortex and to discuss the validity of the Lakshminarayana’s vortex model. Fujita and Takada [4] reported the experimental study on casing treatment to improve the surge margin due to the controlling the tip leakage flow in an axial flow compressor. Recently, as the computer performance and calculating techniques are making remarkable progress, the complex and unsteady flow fields including tip leakage vortex have been clarified using numerical simulation. Furukawa et al. [5] calculated the flow field with tip leakage vortex near stall condition and numerically clarified the phenomenon called vortex breakdown. After then, the researches relating the vortex breakdown to stall inception or rotating instability have been done.

However, the all researches mentioned above were carried out for the “ducted-type” turbomachine, in which the “ducted-type” means the type that the inlet and outlet of turbomachine were connected with the duct, respectively. The number of the

Received July 23 2009; revised May 26 2011; accepted for publication May 26 2011: Review conducted by Prof. Seung Jin Song. (Paper number O09026)
Corresponding author: Norimasa Shiomi, Professor, siomi@me.saga-u.ac.jp

researches for “half-ducted type” is comparatively less than the one for “ducted type”. Fukano et al. [6] experimentally clarified the aerodynamics and aeroacoustic characteristics for the various inlet geometries of a room ventilating fan. Jang et al. [7] experimentally and numerically showed the behavior of tip vortex formed upstream of inlet bellmouth for the cooling fan using at the outer unit of a room air-conditioner. Kato et al. [8] numerically analyzed the effect of tip vortex on fan noise level for a propeller fan without the outer casing. Cai et al. [9] and Shiomi et al. [10] carried out the experimental investigations to clarify the natures of tip vortex of propeller fan.

The final goal of this investigation is to develop the high performance fan, which has high efficiency and low noise level. To archive this goal, a lot of information and knowledge for the internal flow fields with vortices and to design the turbomachines are needed. The purpose of the present investigation is to clarify the features of tip leakage vortex, to find the effect of tip clearance size on the tip leakage vortex, and to provide the useful data for fan design and/or numerical simulation.

2. Experimental Apparatus and Procedure

Figure 1 shows the schematic layout of the test rig. The section geometry of the test rig is rectilinear and its size is 1200 (mm) x 1200 (mm). The flow direction is from right to left in Fig.1. Air flows passing through the test fan, filters, booster fan and outlet chamber, and it flows out through outlet nozzle. The fan performance test was carried out to clarify the fan characteristics and the effect to tip clearance on fan performance. At fan tests, the pressures at outlet chamber and near test fan and the electrical power to run the main motor were measured. As the test rig did not have the throttle, the flow-rate was changed by changing the rotating speed of booster fan. The blade phase is checked using the data of the encoder mounted on the motor shaft.

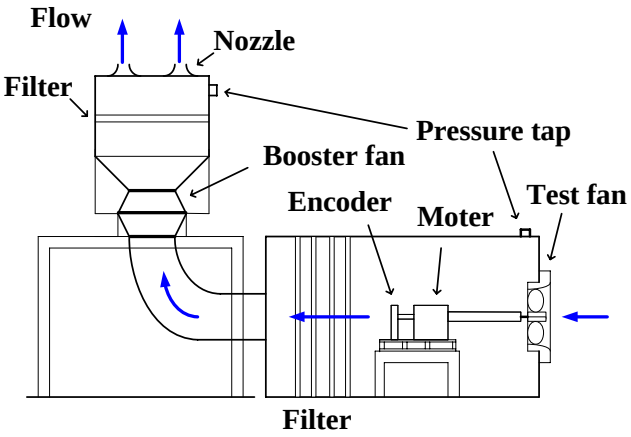

Fig. 1 Schematic layout of test rig

Figure 2 shows the schematic vies of test rotor and the relationship of rotor and outer casing, respectively. The rotor rotating direction of the right figure is counter clock-wise, and the flow direction of the left figure is from left to right as shown in Fig. 2. Test rotor has four blades, its tip diameter is 310 mm and hub-to-tip ratio is 0.32. The clearance between blade tip and outer casing is called as tip clearance (TC). In the present investigation, fan test and internal flow measurement were carried out at three sizes of tip clearance; those were 4mm (2.22% of blade chord length at blade tip), 2mm (1.11% of blade chord length at blade tip) and 1mm (0.55% of blade chord length at blade tip). In this paper, those conditions were shown as TC=4mm, TC=2mm and TC=1mm. As shown in Fig. 2, the outer cashing has a large inlet bellmouth, so in this paper the region of bellmouth is called as “bellmouth region”, and the region of casing covering with the rotor is called as “straight region”, respectively. The condition of TC=4mm

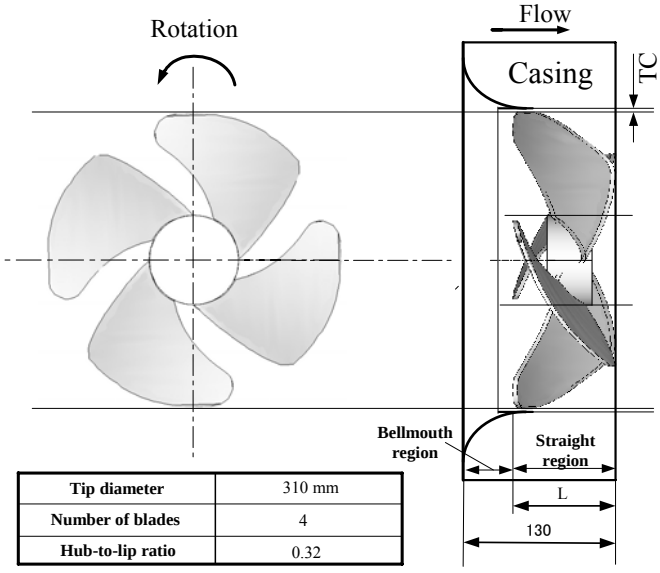

Tip diameter	310 mm
Number of blades	4
Hub-to-lip ratio	0.32

Fig. 2 Schematic view of test fan

was almost the same as the condition of a room ventilation fan on the market. The catalog flow-rate of a room ventilation fan on the market was 1,200 m^3/h when rotor speed was 900 rpm.

The internal flow measurements were done using a 2-dimensional LDV system. Laser source is Argon-ion and maximum laser power is 8 W. The tracer mist is water vapor and its diameter is about 1 to 10 μm.

Figure 3 shows the LDV measurement grids on the meridional plane. The flow direction is from right to left as shown in Fig. 3. The spacing of Z direction of the grid is 5 mm and the one of R direction is 2.5 mm at constant, respectively. The region surrounded by red thick solid line is measurable area in this experiment. As the main target of this study is tip leakage vortex, so the radial measurement location is limited near blade tip and the axial measurement location is limited at the straight region of outer casing. LDV system was set at the upstream of test fan. In this fan, the axial measurement range was limited up to Z13 section because the inlet bellmouth prevented laser beams. And at Z11, Z12 and Z13 location, the data near blade tip region were not captured as the same reason. This location is corresponded with the 66% location of blade chord from blade leading edge.

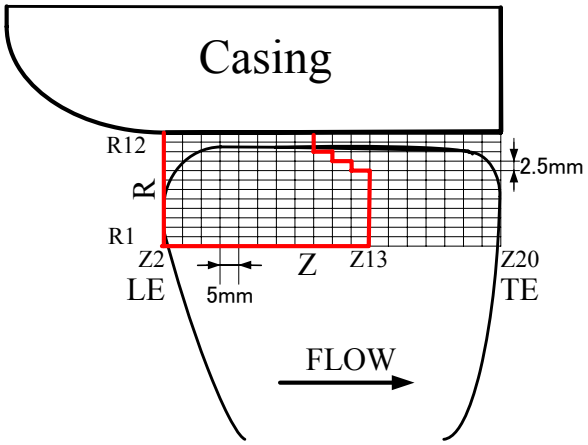

Fig. 3 LDV measurement grid on meridional plane

Figure 4 shows the coordinate system at LDV measurement. The relationship between LDV incidence and rotor blade are also shown. The ordinate is axial direction (Z-dimension) and the abscissa is pitchwise direction of Fig. 4. The flow direction is from top to bottom of the figure and the blade rotating direction is from left to right, respectively. the symbol of "B1" and "B2" mean the "blade 1" and "blade 2", and "PS" and "SS" indicate "pressure surface" and "suction surface", and "LE" and "TE" are "leading edge of blade" and "trailing edge of blade", respectively. The laser beams are inserted into blade passage from blade upstream at the angle of 50 degrees inclined from axial direction, as shown in Fig. 4. The LDV incidence angle is the one approximately parallel to blade angle. Radial and X-directional velocity component were measured at the LDV survey. In this, X-direction is the direction normal to both radial and LDV incidence direction.

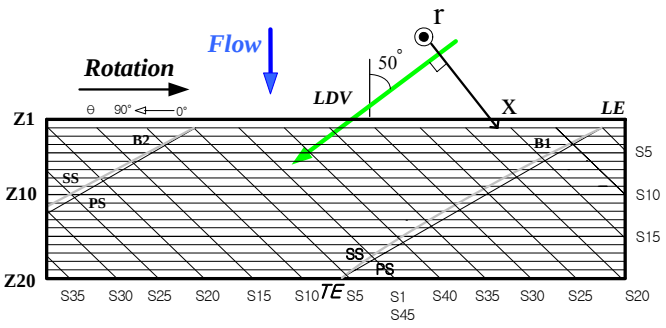

Fig. 4 LDV set-up and measurement coordinate system

LDV system used at this experiment is 2-dimensional. The channel 1, channel 2 and encoder data are recorded at the same time for each measurement point on measurement grid. The minimum valid data number at one measurement is 4,000. The data were rearranged in turn using the encoder data and phase-locked averaged at the interval of 2 degrees. As the angle of one blade spacing is 90 degrees, one blade period is divided into 45 phases. Those phases are call as "Section" and shown as "S", as shown in Fig. 4. Those phase-locked averaging velocity data are shown as the form of velocity vector map for each Section. After then, the vorticity component, ζ_{rx}, on S plane were calculated using the equation as follows.

$$\zeta_{rx} = \frac{\partial V_r}{\partial x} - \frac{\partial V_x}{\partial r} \tag{1}$$

Using those values, the vorticity distribution on each S plane, the trace of vortex core and the distribution of maximum value of

vorticity along S plane were shown.

In the experiment, rotor rotating speed is 900 rpm at constant, and the test Reynolds number based on the blade chord length at tip and blade tip speed is 1.70 x 10^5

3. Experimental Results and Discussions

3.1 Fan Test Results

Figure 5 shows the fan test result at TC=4mm. As the tip clearance of the room ventilation fan on the market was approximately 4 mm, so in this investigation its clearance size was decided as the reference size. The ordinate is pressure-rise coefficient and efficiency, and the abscissa is flow-rate coefficient. The circle symbol in Fig. 5 indicates the pressure-rise coefficient in case of increasing the flow-rate, the triangle symbol indicates the one in case of decreasing the flow-rate, and the diamond symbol indicates the efficiency in case of increasing the flow-rate, respectively. The pressure-rise coefficient, ψ, and the flow-rate coefficient, ϕ, are defined as follows,

$$\psi = \frac{2\,\Delta P}{\rho\, U_t^{\,2}} \tag{2}$$

$$\phi = \frac{Q}{\pi\left(r_t^{\,2} - r_h^{\,2}\right)U_t^{\,2}} \tag{3}$$

, where ΔP is internal pressure-rise, ρ is density of air (kg/m^3), U_t is blade tip speed (m/sec), Q is flow-rate (m^3/sec), r_t is blade tip radius (m) and r_h is hub radius (m).

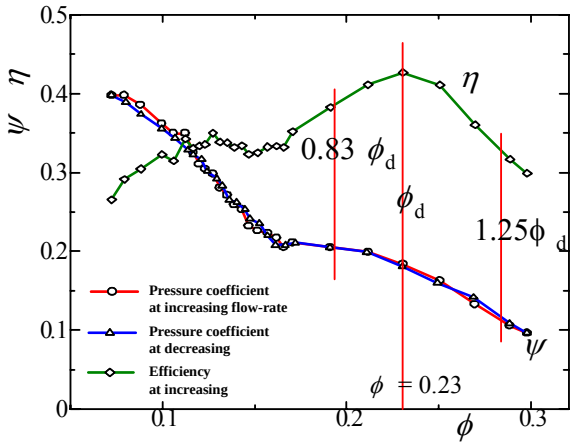

Fig. 5 Fan test result at TC=4mm

Generally, it is known that there is an unstable region with a positive gradient in the pressure – flow-rate curve for axial fan. The unstable region is not clearly observed in the test fan at TC=4mm. It is also found that there is not the hysteresis loop on pressure curve, that is, the pressure curves in both cases of increasing and decreasing the flow-rate is almost the same tendency. It is thought that those reasons are that the tip clearance size of test fan is relatively large and this blade is designed for the low-pressure type. The maximum efficiency was obtained at ϕ = 0.230. Therefore its flow-rate was decided as the reference flow-rate, ϕ_d.

Figure 6 shows the pressure-rise – flow-rate curves of fan test for three tip clearance sizes in case of increasing flow-rate. The ordinate is pressure-rise coefficient and the abscissa is flow-rate coefficient. The symbol of black circle is the case of TC=4mm, red circle is TC=2mm and blue circle is TC=1mm, respectively.

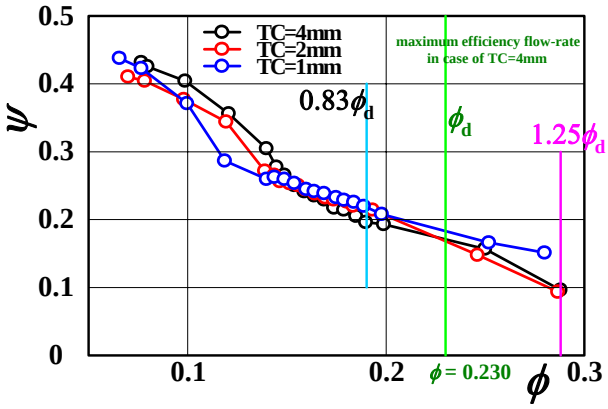

Fig. 6 Fan test result at TC=4mm

It is found from Fig. 6 that the overall tendency of pressure – flow-rate curves dose not have large difference, i.e., there is no unstable characteristic with a positive gradient and no hysteresis loop. Observing the curves in details, pressure coefficient becomes high at large flow-rate region, as the size of tip clearance becomes small. Although it is not clear, the point where the slope of pressure curve changes, as likely stall point, also shifts to small flow-rate region, as the size of tip clearance becomes small. Those characteristics are desirable for general fan performance.

In the present study, the detail flow measurements using LDV were performed at three flow conditions for each tip clearance. As the efficiency becomes the maximum value at $\phi = 0.23$, this flow-rate was decided as the reference flow-rate ϕ_d. And, the flow fields were measured at large flow-rate condition, $\phi = 1.25\phi_d$, reference flow-rate condition, $\phi = \phi_d$ and small flow-rate condition, $\phi = 0.83\phi_d$.

3.2 Basic Process of tip leakage vortex developing

At first, the basic process of tip leakage vortex developing, i.e., vortex generation, growth-up, weakness and/or disappearance, of test fan is introduced in case of reference tip clearance size, TC=4mm, at reference flow-rate condition, $\phi = \phi_d$.

Figure 7(a-d) show the V_x-V_r velocity vector maps on S plane in case of TC=4mm at $\phi = \phi_d$. The ordinate is radial direction and the abscissa is x-direction, respectively. The blade tip speed, U_t, is indicated in each figure. Those figures correspond to the vortex generation, growth-up, expansion, and weakness process, respectively.

In the case of TC=4mm at $\phi = \phi_d$, clear vortex is observed on the S12 plane for the first time. However, its location is near the point where the bellmouth region and straight casing region of outer casing is connected, and a little far from the blade. Therefore, it is thought that the bellmouth play an important role on the forming this vortex. Its vortex is gradually growing up from the S12 plane to the S26 plane, and it rapidly apart from blade SS. The shape of vortex is confirmed up to the S43 plane expanding the area of tip leakage vortex. After then, the shape of vortex is gradually declining on the S50 plane. Finally, on the S57 plane, which equals to the S12 plane, the shape of vortex is not observed. It means that the tip leakage vortex in case of TC=4mm at $\phi = \phi_d$ disappears inside the blade passage, not flowing out to downstream of rotor.

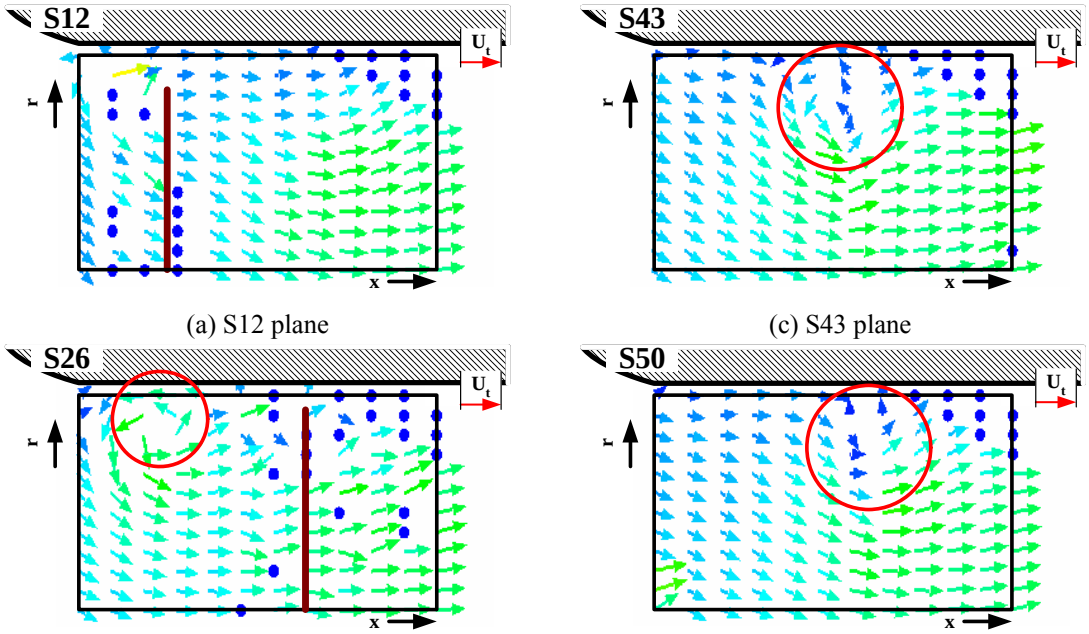

(a) S12 plane (c) S43 plane

(b) S26 plane (d) S50 plane

Fig. 7 Velocity vector maps on S plane in case of TC=4mm at $\phi = \phi_d$

3.3 Effect of flow-rate condition on vortex feature

In this section, the effect of flow-rate condition on the vortex features is shown using V_x-V_r velocity vector maps on S plane and its differences are discussed in case of the reference tip clearance, TC=4mm.

Figure 8(a-c) shows the V_x-V_r velocity vector maps on S plane in case of TC=4mm at $\phi = 1.25\phi_d$. The ordinate is radial direction and the abscissa is x-direction, respectively. The blade tip speed, U_t, is indicated in each figure. These figures correspond to the vortex generation, growth-up and weakness process, respectively.

In the case of TC=4mm at $\phi = 1.25\phi_d$, the vortex is observed on the S15 plane for the first time, that is, its section is more downstream section than the one where the vortex is observed at $\phi = \phi_d$. It is also found that the vortex location is near blade tip. Therefore, it is thought in this case that the tip clearance flow have a large effect on the forming the vortex. Its vortex is gradually growing up from the S15 plane to the S24 plane. However, the location of the vortex is on blade SS near blade tip. This is the point different from the result at $\phi = \phi_d$. After then, the vortex is gradually weakened expanding the area of the vortex, and near S38 plane it flows out to downstream region.

Figure 9(a-c) shows the V_x-V_r velocity vector maps on S plane in case of TC=4mm at $\phi = 0.83\phi_d$. The ordinate is radial direction and the abscissa is x-direction, respectively. The blade tip speed, U_t, is indicated in each figure. These figures correspond

to the flow pattern before the vortex is generated, vortex generation and development process, respectively.

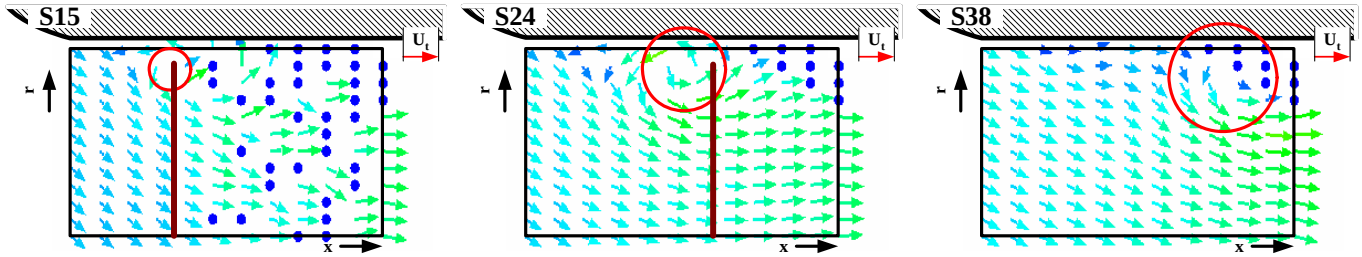

(a) S15 plane (b) S24 plane (c) S38 plane

Fig. 8 Velocity vector maps on S plane in case of TC=4mm at $\phi = 1.25\phi_d$

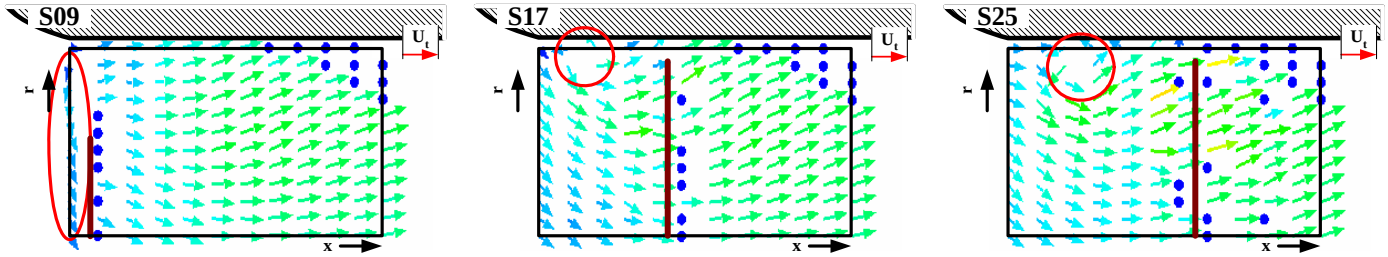

(a) S9 plane (b) S17 plane (c) S25 plane

Fig. 9 Velocity vector maps on S plane in case of TC=4mm at $\phi = 0.83\phi_d$

In the case of TC=4mm at $\phi = 0.83\phi_d$, firstly, on the S9 plane the strong radial inward flow on blade SS near blade tip is observed. However, the vortex is not confirmed at this section. Secondary, on the S17 plane, the clear vortex is observed for the first time. Its location is near the point where the bellmouth region and straight casing region of outer casing is connected and a little far the blade. Its vortex stays around there even on the S25 plane and the size of vortex on the S25 plane is almost the same size on the S17 plane. It means that this vortex moves almost circumferentially. After then, its vortex disappears inside the blade passage.

From these results, it is found in case of TC=4mm that the tip leakage vortex is generated only at $\phi = 1.25\phi_d$. Although the vortex is generated at other flow-rate condition, $\phi = \phi_d$ and $\phi = 0.83\phi_d$, it is mainly formed due to the effect of not the tip leakage flow but the bellmouth. It is also found that the vortex flows out to downstream only at $\phi = 1.25\phi_d$ whereas the vortex at $\phi = \phi_d$ and $\phi = 0.83\phi_d$ moves to almost circumferential direction and disappears inside the blade passage, not flowing out to downstream region.

3.4 Effect of tip clearance on vortex feature

In this section, the effect of tip clearance size on the vortex features is shown using V_x-V_r velocity vector maps on S plane and its differences are discussed for the large flow-rate condition, $\phi = 1.25\phi_d$.

Figure 10(a-c) shows the V_x-V_r velocity vector maps on S plane in case of TC=2mm at $\phi = 1.25\phi_d$. The ordinate is radial direction and the abscissa is x-direction, respectively. The blade tip speed, U_t, is indicated in each figure. These figures show the same section in Fig. 8 in case of TC=4mm at $\phi = 1.25\phi_d$.

In case of TC=2mm, firstly, the clear vortex is not still observed on the S15 plane, but the flow disturbance similar to vortex exists near blade tip on blade SS. It is thought that this disturbance is rolling up and tip leakage vortex is formed, that is, the roll-up point of tip leakage vortex in case of TC=2mm shifts more downstream region than the one in case of TC=4mm. Secondary, on the S24 plane, the clear vortex is confirmed. Its location is a little far from the blade SS. Therefore, it is found that the tip leakage vortex in this case moves to more circumferential direction than the one in case of TC=4mm. Finally, on the S38 plane, the vortex is broken in this case. It is not clear vortex. It is also found that the area of vortex does not so enlarge compared with the result in Fig. 8(c).

Figure 11(a-c) shows the V_x-V_r velocity vector maps on S plane in case of TC=1mm at $\phi = 1.25\phi_d$. The ordinate is radial direction and the abscissa is x-direction, respectively. The blade tip speed, U_t, is indicated in each figure. These figures show the same section in Fig. 8 in case of TC=4mm at $\phi = 1.25\phi_d$.

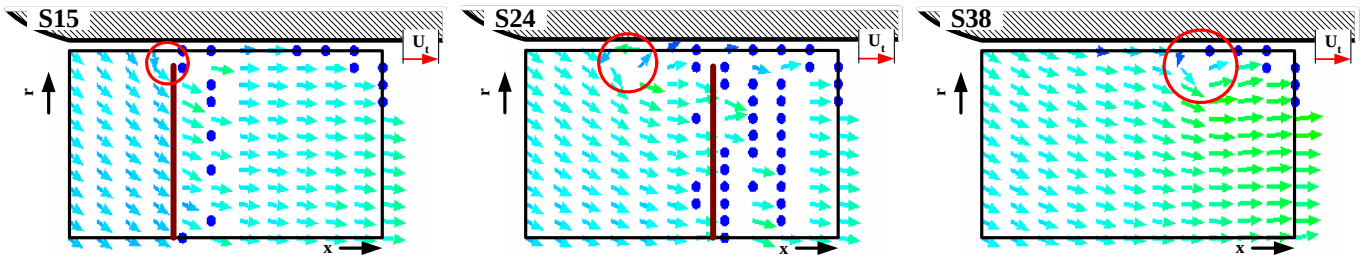

(a) S15 plane (b) S24 plane (c) S38 plane

Fig. 10 Velocity vector maps on S plane in case of TC=2mm at $\phi = 1.25\phi_d$

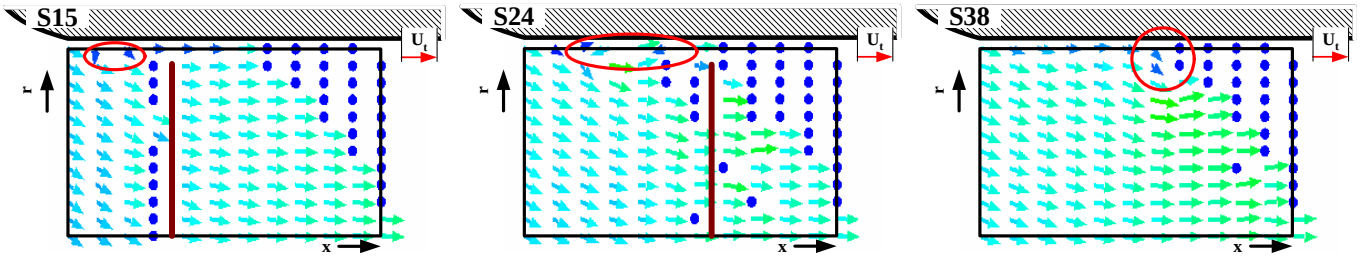

(a) S15 plane (b) S24 plane (c) S38 plane

Fig. 11 Velocity vector maps on S plane in case of TC=1mm at $\phi = 1.25\phi_d$

In case of TC=1mm, it is found at all sections shown in Fig. 11 that the clear vortex is not confirmed. On the S15 plane, the flow disturbance occurs at the location between the connecting point with bellmouth and straight casing region and rotor blade. Whether this disturbance is caused by the effect of bellmouth or it is caused by the effect of tip clearance flow cannot be clarified only from this result. Similar disturbance also exists on the S24 plane, but it cannot be stated that this disturbance is the vortex. And, the effect of this disturbance is seen on the S38 plane.

From these results, it is found at the large flow-rate condition that the tip leakage vortex is generated in case of TC=2mm. It is not, however, stated that the vortex exist in case of TC=1mm. It is shown that the tip leakage vortex in case of TC=2mm has almost the same features in case of TC=4mm.

3.5 Vortex Trace

In this section, the traces of vortex core are shown and the effects of flow-rate and tip clearance size on vortex trace are discussed. The vortex trace is drawn based on the vorticity. Therefore, the vorticity distribution on S plane is obtained to check the calculation of vorticity component.

Figure 12(a)(b) show the velocity vector map and the vorticity distribution on S24 plane in case of TC=4mm at f=1.25fd. The ordinate is radial direction and the abscissa is x-direction, respectively.

From this result, it is found that the value of vorticity shown in Fig. 12(b) becomes high at the region where the vortex exists shown in Fig. 12(a). Almost the same results are obtained for other flow condition and tip clearance size. The location of vortex core on each S plane is decided from the location of maximum value of vorticity distribution on each S plane. The vortex trace in

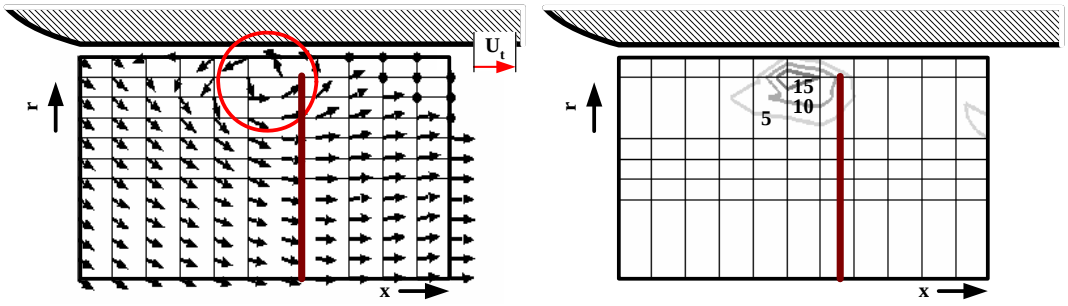

(a) V_x-V_r velocity vector map (b) Vorticity distribution

Fig. 12 Velocity vector map and vorticity distribution on S24 plane in case of TC=4mm at $\phi = 1.25\phi_d$

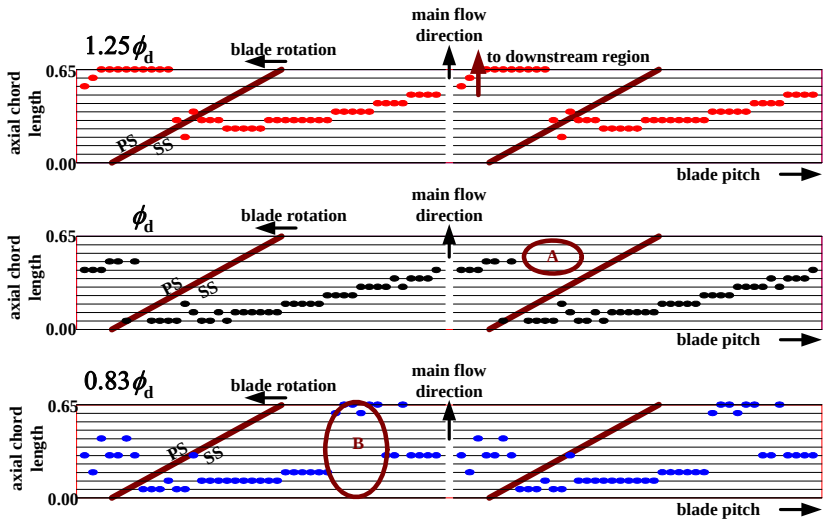

Fig. 13 Vortex traces in case of TC=4mm at three flow-rate conditions

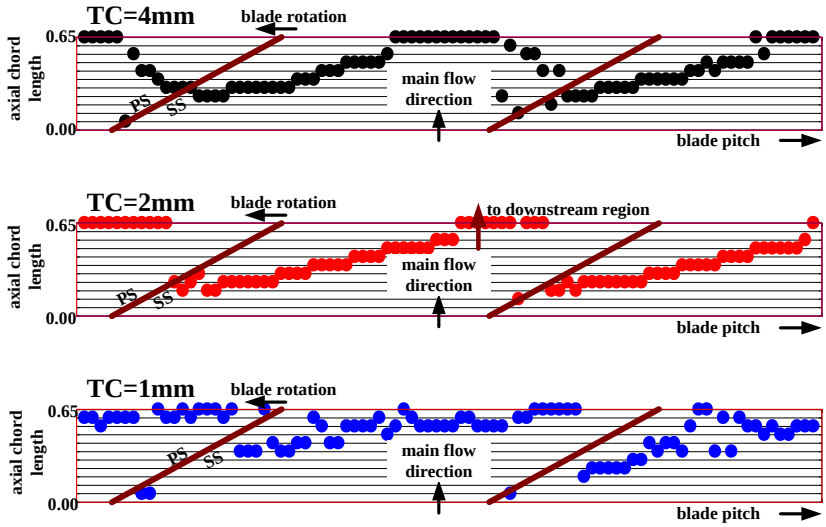

Fig. 14 Vortex traces at $\phi = 1.25\phi_d$ for three tip clearance sizes

case of TC=4mm at three flow-rate conditions are shown in Fig. 13.

The top figure in Fig. 13 shows the vortex trace for $\phi = 1.25\phi_d$, the middle figure shows for $\phi = \phi_d$ and the bottom figure shows for $\phi = 0.83\phi_d$. The ordinate is non-dimensional axial chord length and the abscissa is pitchwise direction, respectively. The slant bold lines in each figure indicate the blade. "PS" and "SS" in figures are "blade pressure surface" and "blade suction surface", respectively. The flow direction is from bottom to top for each figure and blade rotating direction is from right to left, as shown in figure.

It is found at $\phi = 1.25\phi_d$ (top figure in Fig. 13) that tip leakage vortex starts at 25% chord length from blade leading edge. On the other hand, at $\phi = \phi_d$ and $\phi = 0.83\phi_d$, it starts at 5% chord length from blade leading edge. As its location is near bellmouth region, it is difficult to distinguish whether its vortex is caused by the effect of bellmouth or it caused by the tip leakage flow only from these data. It is found at $\phi = 1.25\phi_d$ that the tip leakage vortex flows out to downstream region. On the other hand, at $\phi = \phi_d$, the vortex cannot have been seen at the location "A" in middle figure of Fig. 13. The main reason of this is that the vortex moves to the region that cannot be measured, so whether its vortex disappears or it exists still is unknown. However, if its vortex exists, it is thought that its vortex goes to the blade PS of next blade because of inclination of vortex trace. At $\phi = 0.83\phi_d$, the vortex disappears at the location "B" in bottom figure of Fig. 13. It is thought that the reason of this disappearance is vortex break-down.

Figure 14 shows the vortex trace for each tip clearance size at $\phi = 1.25\phi_d$. The top figure in Fig. 14 shows the result for TC=4mm, the middle figure shows for TC=2mm and the bottom figure shows for TC=1mm. The view of Fig. 14 is the same one of Fig. 13.

It is found that the tip leakage vortex exists in case of TC=2mm but it does not exist in case of TC=1mm. The starting point of tip leakage vortex in case of TC=2mm shifts to more upstream region than the one in case of TC=4mm. And, its trace of TC=2mm moves to more circumferential direction than the one of TC=4mm. It is thought that its reason is that the leakage jet becomes strong as the tip clearance becomes small and the pressure difference between blade PS and SS becomes large. On the other hand, in case of TC=1mm, the trace of vortex cannot be decided from this results. As the clear vortex was not confirmed at the velocity vector map, it is thought that the vortex not exist in this clearance size even at the large flow-rate condition.

From these results, in case of TC=4mm at the large flow-rate condition, the tip leakage vortex is formed and its vortex flow out to downstream region. At the reference flow-rate condition, the vortex exists, but it is difficult to judge whether its vortex is tip leakage vortex or not. Its vortex does not flow out to downstream region, but circumferentially moves to the next blade. At the small flow-rate condition, the vortex exists, too. However, it is also difficult to judge whether its vortex is tip leakage vortex or not. Its vortex disappears inside blade passage probably due to the vortex break down. At the large flow-rate condition, the tip leakage vortex exists in case of TC=2mm. As the tip clearance becomes small, the starting point of tip leakage vortex shifts to upstream and the inclination of the vortex trace becomes more circumferentially.

3.6 Vorticity Distribution along S Planes

In this section, vorticity distributions are shown and the effects of flow-rate and tip clearance size on vortex features are discussed. The maximum value of vorticity on each S plane are picked up and rearranged along S number in Fig. 15.

In Fig. 15 the ordinate is vorticity and the abscissa is S plane's number, respectively. The black marks in Fig. 15 are the results of $\phi = \phi_d$, the red marks are the one of $\phi = 1.25\phi_d$ and the blue marks are the one of $\phi = 0.83\phi_d$, respectively. As the data varies widely, so the discussion is done only for the general tendency of vortex feature.

The maximum value of vorticity becomes the largest at $\phi = 1.25\phi_d$, but its width is narrow. In this case, the vorticity rapidly increases and after then rapidly decreases. Its reason is thought that tip leakage vortex in this case flows out to downstream region of measurable area of LDV and do not stay in measurable area of LDV. The vorticity distribution of $\phi = \phi_d$ gradually decreases than the one of $\phi = 1.25\phi_d$. Therefore, it is thought that the vortex in this case stays in the measurable area of LDV, that is, the vortex trace of this case inclines more circumferential direction than the one at $\phi = 1.25\phi_d$. At $\phi = 0.83\phi_d$, the vorticity distribution exists, i.e., its curve has a peak. However, its peak value is lower than the ones at $\phi = 1.25\phi_d$ and $\phi = \phi_d$. And, its width becomes a

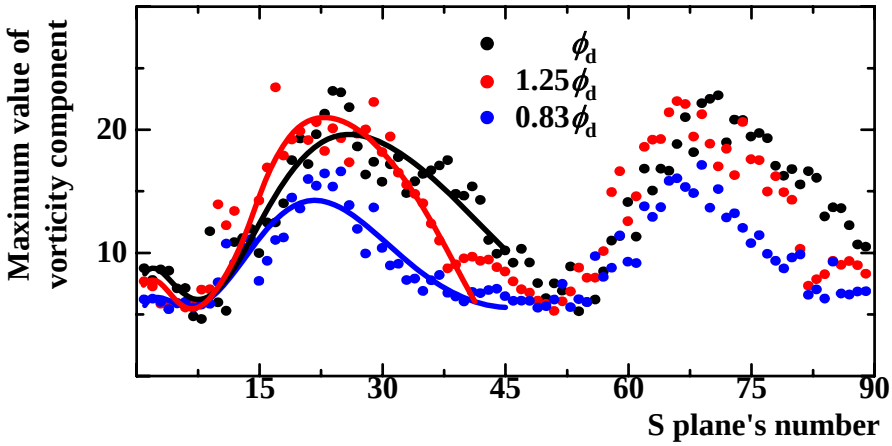

Fig. 15 Maximum vorticity distribution along S plane in case of TC=4mm at three flow-rate condition

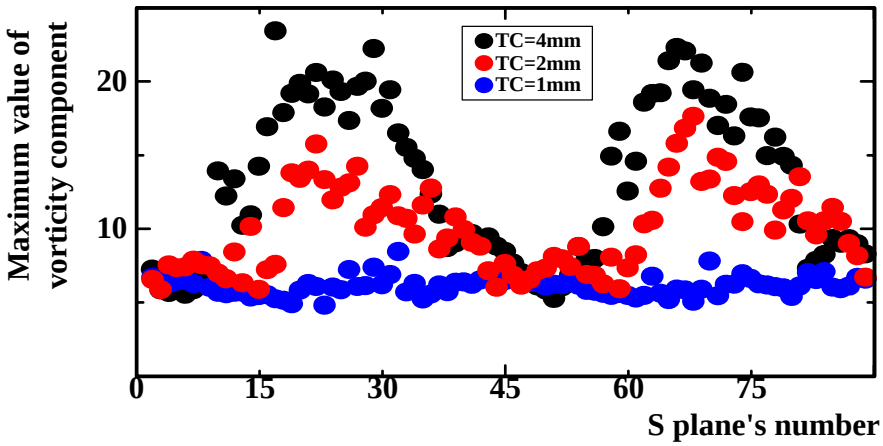

Fig. 16 Maximum vorticity distribution along S plane in three tip clearance sizes at $\phi = 1.25\phi_d$

narrow. It means that the vortex exists in this case, but its vortex is small and weak.

Figure 16 shows the vorticity distributions along S plane at $\phi = 1.25\phi_d$ in three tip clearance sizes. The ordinate and the abscissa is the same ones of Fig. 15. The blade marks indicate the result for TC=4mm, the red marks indicate for TC=2mm and the blue marks indicate for TC=1mm, respectively.

It is found from Fig. 16 that the vorticity distribution exists in case of TC=4mm and TC=1mm, but it does not exist in case of TC=1mm. It is also found that the peak value of vorticity in case of TC=4mm is larger than the one in case of TC=2mm. Therefore, as the tip clearance becomes large, a stronger vortex occurs in this fan. And, as the tip clearance becomes very small, the vortex cannot be formed.

From these results, it is found that the vorticity becomes large as the flow-rate increases at the same tip clearance size. At the large flow-rate condition, the vorticity rapidly increases after the tip leakage vortex is formed. It is also found that the vorticity becomes large as the tip clearance becomes large. When the tip clearance becomes very small, the tip leakage vortex is not observed in this experiment.

4. Conclusions

The internal flow fields including the vortex in a half-ducted axial fan with large bellmouth were measured using LDV, and the effects of flow-rate condition and tip clearance size on fan performance and vortex were investigated. The main conclusions are as follows.

1. The test fan does not have the unstable characteristic with a positive gradient and the hysteretic characteristic even at the smallest tip clearance condition. As the tip clearance becomes small, the pressure-rise becomes high at the large flow-rate condition and the stall point shifts to low flow-rate region.
2. When the vortex exists, the process of generation, development, declination is almost the same process at all tip clearance sizes and flow-rate conditions.
3. The clear tip leakage vortex occurs only at the large flow-rate condition for TC=4mm and 2mm. It cannot be judged whether other vortex occurred at reference and small flow-rate condition for TC=4mm and TC=2mm is tip leakage vortex or not. And for TC=1mm, the vortex does not exist even at the large flow-rate condition.
4. The tip leakage vortex in case of TC=2mm becomes small and weakens compared with the one in case of TC=4mm, although the structure and behavior of tip leakage vortex in case of TC=2mm is similar to the one in case of TC=4mm. Also, the vortex trace in case of TC=2mm inclined toward more tangential direction compared with the one in case of TC=4mm.

5. Tip leakage vortex flows out to downstream region only at the large flow-rate condition for TC=4mm and 2mm. The vortex for other flow-rate condition and tip clearance size does not flow out to downstream region. It moves to circumferential direction or disappears inside the blade passage.
6. Tip leakage vortex is rapidly growing up. As the flow-rate increases and tip clearance becomes large, the vortex becomes strong.

Nomenclature

L	Blade chord length on meridional plane [m]	TE	Blade Trailing Edge
LDV	Laser Doppler Velocimetry	U_t	Blade tip speed [m/sec]
LE	Blade Leading Edge	V_r	Radial velocity component [m/sec]
Q	Flow-rate [m^3/sec]	V_x	x-directional velocity component [m/sec]
ΔP	Pressure difference at outlet nozzle	X	x-direction
PS	Blade Pressure Surface	Z	Axial measurement location at LDV grid
R	Radial direction	ϕ	Flow-rate coefficient
R	Radial measurement location at LDV grid	ϕ_d	Reference flow-rate at measurement
S	Section (S1, S2…)	η	Efficiency
r_h	Radius at hub [m]	ρ	Density of air [kg/m^3]
r_t	Radius at tip [m]	ψ	Pressure coefficient
SS	Blade Suction Surface	ζ_{rx}	Vorticity component on S plane
TC	Tip Clearance [mm]		

References

[1] Inoue, M., 1997, "Vortex and Turbomachinery," Procs. of 5th Asian International Conference on Fluid Machinery, Seoul (Korea), pp. 117-131.

[2] Lakshminarayana, B., 1970, "Methods of Predicting the Tip Clearance Effects in Axial Flow Turbomachinery," Trans. ASME, Journal of basic Engineering, 92, pp. 467-482.

[3] Inoue, M., Kuroumaru, M., Furukawa, M., Kawashima, Y., Shen, W., 1985, "Experimental Study on Tip Leakage Flow in Axial Flow Rotating Blades," Trans. JSME, B, 51-468, pp. 2545-2553(in Japanese).

[4] Fujita, H., 1983, "A Study on Configurations of Casing Treatment for Axial Flow Compressors," Trans. JSME, B, 49-448, pp. 2945-2953(in Japanese).

[5] Furukawa, M., Saiki, K., Yamada, K., Inoue, M., 2000, "Anomalous Flow Phenomena Due to Breakdown of Tip Leakage Vortex in an Axial Compressor Rotor at Near-Stall Condition," Trans. JSME, B, 66-644, pp. 1029-1037 (in Japanese).

[6] Fukano, T., Tukuhara, M., Kawagoe, K., Hara, Y., Kinoshita, K., 1990, "Experimental Study on the Noise Reduction of a Propeller Fan: 1st Report, Aerodynamic Characteristic," Trans. JAMS, B, 56-531, pp. 3378-3382(in Japanese).

[7] Jang. C. M., Furukawa, M., Inoue, M., 2001, "Analysis of Vortical Flow Field in a Propeller- Fan by LDV Measurement and LES – Part 1: Three-Demensional Vortical Flow Structures," Trans. ASME, Journal of Fluids Engineering, 123, pp. 748-754.

[8] Kato, C., Shishido, S., Miyazawa, M., Yoshiki, H., Ito, H., Tsubota, H., 2002, "Numerical Prediction of Aerodynamic Noise Radiated from a Propeller Fan," Procs. of 5th JSME-KSME Fluids Engineering Conference, Nagoya(Japan), pp. 522-527.

[9] Cai, W. X., Shiomi, N., Sasaki, K., Kaneko, K., Setoguchi, T., 2002, "Visualization of Tip Vortex Flow in an Open Axial Fan by EFD," Journal of Visualization, 5-3, pp.293-300.

[10] Shiomi, N., Kaneko, K., Cai, W. X., Sasaki, K., Setoguchi, T., 2003, "Tip Vortex Feature in an Open Axial Fan," Turbomachinery, 31-9, 545-553(in Japanese).